Some questions related to CFD modeling of pressurized tank burst in road tunnels

Guillaume Lecocq, Laure Heudier, Benjamin Truchot, Antoine Mos, Christophe Willmann

Some questions related to CFD modeling of pressurized tank burst in road tunnels

Guillaume Lecocq [a], Laure Heudier [a], Benjamin Truchot [a], Antoine Mos [b]& Christophe Willmann [b]

[a] INERIS (Verneuil-en-Halatte, France)
[b] CETU (Bron, France)

E-mail: *guillaume.lecocq@ineris.fr*

Abstract

The current paper focuses on high-pressure reservoirs and the consequences of their potential burst, related to scenarios of thermal or mechanical aggressions, in tunnels.

CFD (Computational Fluid Dynamics) modeling can be used to account for the effects of such scenarios. An intrinsic advantage of such an approach consists in integrating the specific geometrical effects (tunnel walls, presence of vehicles) on the pressure wave propagation.

To meet such an objective, experimental data are required to offer an opportunity for validation. Data from the literature and new ones from INERIS are detailed in this paper, with their strengths and weaknesses to identify relevant test cases for CFD.

Phenomenological tools are tested against experimental cases of bursting tank in a free field to evaluate their prediction capability for pressure. These tools could be used along with CFD in a global modeling framework.

CFD is tested against fictitious free-field cases, investigating the effect of the thermodynamic model on the results. The numerical method for propagating the pressure wave in realistic tunnels is also studied.

Keywords: tank burst, pressure effects, CFD, phenomenological tools

Introduction

To meet the objective of reducing the transportation impact on the global warming, car manufacturers currently develop new technologies. According to this change, the propulsion of vehicles crossing tunnels is expected to be more and more varied in a next future with Batteries, Fuel Cells or spark-ignition engines using either Natural Gas or Hydrogen. Currently, those two gases, Hydrogen and Natural Gas, are stored at a gaseous state under high pressure, up to 700 bar. The presence of such reservoirs in tunnels raises new risks that should be finely considered by technical experts and regulators.

A first specificity of such bursts in confined geometries is the existence of a reflection zone, close to the bursting capacity, leading to the formation of a planar pressure wave. The intensity of this latter decays much more slowly than in free field. Also, vehicles can be present and influence the pressure wave propagation.

As CFD intrinsically accounts for geometrical effects, this method appears attractive for dealing with these scenarios. Nevertheless, confronting CFD computations to reference test cases is needed to define a modeling strategy. Available experimental data are first listed and described. Phenomenological tools are then tested against some points of the database. These tools could be used along with CFD for getting a reference solution for example. CFD computations are also compared with free-field and tunnel burst tank cases.

1. Experimental data

1.1. Tunnel cases

The data of the literature produced in the framework of experimental campaigns in tunnels is given in the Table below. They are mainly the measurements from Kudriakov et al. (2022) in a disused 507 m long road tunnel. Original data obtained by INERIS in its test tunnel are also supplied. This tunnel cross section is about 10 m² and its length of about 80 m.

***Table 1**. Dataset for the tank burst in tunnel. The tests performed at INERIS are in italics. Reference [1] stands for (Blanc-Vannet et al., 2019), [2] for (Kudriakov et al., 2022) with second pressure peak in brackets, [3] for (Ruban et al., 2012) and [4] for (INERIS, 2012)*

Gas	Bottle type	Aggression mode	Volume (L)	Initial pressure (bar)	Rupture pressure (bar)	Brode energy (ideal gas law) (MJ)	Pressure measurements	Ref.
N2	*IV*	*Fire*	*19*	*700*	*706*	*3.3*	*At 5m: 220mbar*	*[1]*
N2	*IV*	*Fire*	*19*	*700*	*715*	*3.4*	*At 5m:287mbar*	*[1]*
N2	*IV*	*Fire*	*36*	*700*	*749*	*6.7*	*At 5m: 433mbar*	*[1]*
N2	*IV*	*Fire*	*36*	*700*	*716*	*6.4*	*At 5m: 399mbar*	*[1]*
N2	*IV*	*Fire*	*19*	*525*	*585*	*2.8*	*At 5m: 399mbar*	*[1]*
N2	*IV*	*Fire*	*19*	*700*	*714*	*3.4*	*At 5m: 377mbar*	*[1]*
He	IV	Detonation belt	78	650	650	7.7	At 30 m: 98 mbar / 50m: 85 mbar 80 m: 72 mbar / 110m: 68 mbar 140 m: 61 mbar / 170 m: 55 mbar	[2]
H_2	IV	Detonation belt	78	520	520	10.1	At 30 m: 207 mbar (271 mbar) 50m: 180 mbar (243 mbar) 80 m: 160 mbar / 110m: 205 mbar 140 m: 202 mbar / 170 m: -	[2]
H_2	IV	Detonation belt	78	610	610	11.9	At 30 m: 187 mbar (218 mbar) 50m: 180 mbar (225 mbar) 80 m: 151 mbar (204 mbar) 110m: 205 mbar (336 mbar) 140 m: 301 mbar / 170 m: 179 mbar	[2]
He	*IV*	*Fire*	*36*	*350*	*378*	*2.1*	*At 30 m: 187 mbar*	*[3]*
He	*IV*	*Fire*	*36*	*700*	*703*	*3.8*	*At 30 m: 248 mbar*	*[3]*
He	*III*	*Fire*	*17*	*718*	*881*	*2.3*	*At 19 m: 140 mbar / 24 m: 159 mbar / 29 m: 152 mbar*	*[3]*
He	*IV*	*Mechanical impact*	*2.4*	*698*	*698*	*0.25*	*At 1 m: 150 mbar / 5 m: 50 mbar*	*[4]*
He	*IV*	*Mechanical impact*	*2.4*	*693*	*693*	*0.25*	*At 2 m: 142 mbar / 5 m: 67 mbar*	*[4]*

A CFD method for modeling high-pressure tank bursts should be regarded on cases with increasing physical complexity for validation purpose. Then, a modeling work should first address the burst of non-reacting gas tanks. Indeed, the fireball was proved to contribute to the pressure effects (Molkov et al., 2015). Furthermore, the aggression mode is of importance as it impacts the discharge of the pressure wave. In free field, most reservoirs of the literature contain hydrogen and are thermally aggressed, making these cases hard to address with CFD. A CFD method was nevertheless previously proposed by Molkov et al. (2021) for such cases.

The results obtained recently by Kudriakov et al. (2022) are interesting as the way the pressure discharge is obtained is partially controlled, non-reacting gases are used, and numerous measuring

points were exploited. Nevertheless, there are no pressure measurements around the tank (between the tank and the first wall met by the pressure wave for example).

When the purpose is to assess the behavior of modeling tools, it is wished to check they could reproduce the pressure field from the source to an observer location. Some campaigns show only one measurement point, making them difficult to be used for validating tools.

The graph below is built from the data of Table 1. It plots the peak pressure versus the reduced distance λ, which writes: $\lambda = r/m_{TNT}^{1/3}$. r is the distance between the pressure source and the sensor and m_{TNT} is the TNT equivalent. This latter is deduced from E, the tank rupture energy, closed with the expression of Brode (1959): $E = \Delta p.V/(\gamma - 1)$. V is the tank volume, Δp is the rupture pressure and γ is the heat capacity ratio of the stored gas. An ideal gas behavior is assumed in this formula.

A free-field pressure decay is computed with the PROJEX tool (Heudier, 2013), relying on the Multi-Energy method abacus (Van der Berg, 1984). The severity is then set to 10 and the explosion energy is calculated with the Brode formula. The comparison shows that for a given explosion energy, the available experimental data describe either the spherical pressure wave expansion or the planar wave propagation, but not the whole propagation process.

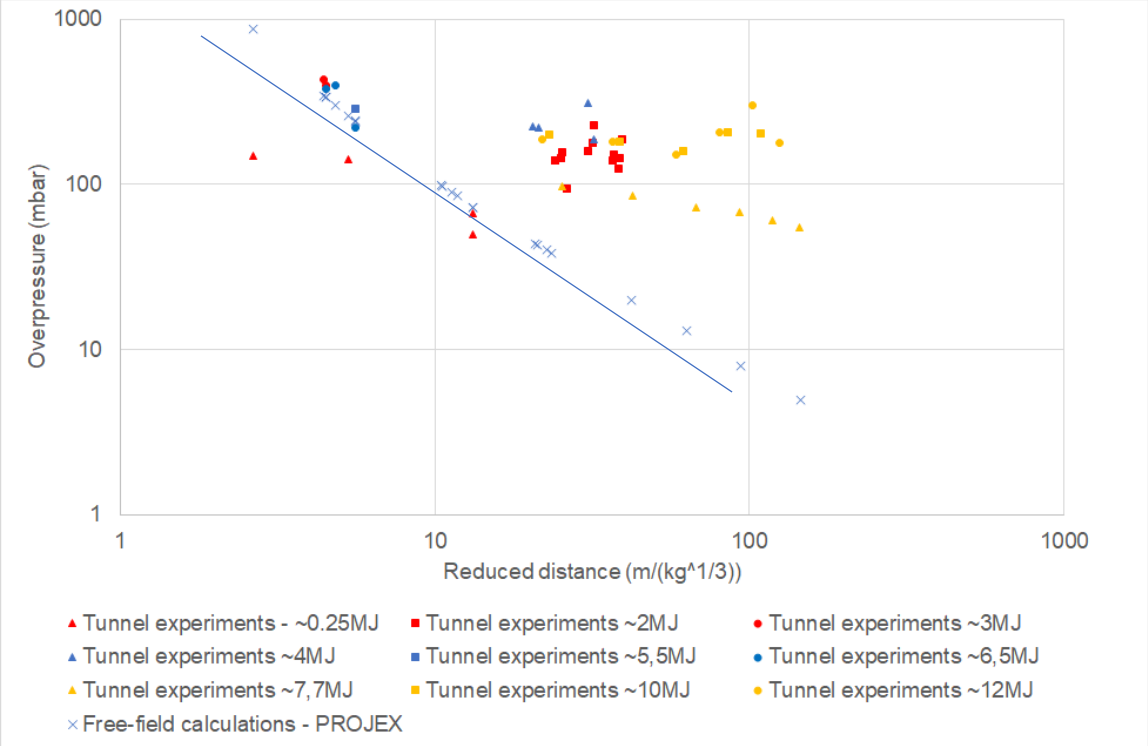

Fig. 1. *Overpressure peaks in case of tank burst in tunnel (experiments) and in free field (calculations). The blue line approximates the PROJEX results.*

The database is not sufficient for testing CFD. Tank burst cases in free field are then regarded in the next section.

1.2. Free-field cases

The data found in the literature related to tests of high-pressure tanks bursting in free field are detailed in Table 2. This latter contains also original data produced by INERIS.

The overpressure measurements in Fig. 2 show that several values of overpressure peaks can be retained, depending on the analysis of the measured signal. That's why, in Table 2, for some tests, several values of overpressure peaks are indicated for the same sensor. For this reason, it is preferable

to have the overpressure signals and not only the peak values when trying to assess the performance of modeling tools such as phenomenological or CFD based ones.

***Table 2**. Dataset for the tank burst in free field. For the data [(1)], the bottle was surrounded by four concrete walls that could have impacted the measured value. Furthermore, the bottle moved when bursting making it difficult to know the real distance between the sensor and the bottle. The tests performed at INERIS are in italics. Reference [1] stands for (Zalosh et al., 2005), [2] for (Shen et al., 2018), [3] for (Tamura et al., 2006), [4] for (Chaineaux, 2000), [5] for (INERIS, 2010) and [6] for (Blanc-Vannet et al., 2019)*

Gas	Bottle type	Aggression mode	Volume (L)	Initial pressure (bar)	Rupture pressure (bar)	Pressure measurements	Ref.
H_2	IV	Fire	72.4	343	357	On the bottle axis, at 4.2m: 650 mbar On the normal axis, at 1.9m: 3 bar / 4.2 m: 830 mbar, 6.5m: 410 mbar	[1]
H_2	III	Fire	165	350	440	No pressure measurement. Bottle projected 200 m away	[2]
H_2	IV	Fire	35	700	945	At 5 m: 1.1 bar / 10 m: 234 mbar	[3]
H_2	III	Fire	36	700	995	At 5 m: 743 mbar / 10 m: 234 mbar	
H_2	*N/A*	*Detonating cord*	*9*	*700*	*700*	*Axis 1, at 10 m: 96 mbar / 15 m: 58 mbar* *Axis 2, normal to axis 1:* *at 10 m: 110 mbar / 15 m: 64 mbar*	*[4]*
H_2	*IV*	*Fire*	*2.4*	*481*	*600*	*At 5 m: 58-68 mbar / 10 m: 30-36 mbar*	*[5]*
H_2	*IV*	*Fire*	*2.4*	*525*	*673*	*At 5 m: 58-75 mbar / 10 m: 32 mbar*	
H_2	*IV*	*Fire*	*2.4*	*700*	*827*	*At 5 m: 61-69-78 mbar / 10 m: 38 mbar*	
H_2	*IV*	*Fire*	*2.4*	*700*	*854*	*At 5 m: 71-80-104 mbar / 10 m: 41-53 mbar*	
N_2	*IV*	*Fire*	*19*	*700*	*722*	*At about 1 m: 1 bar[(1)]*	*[6]*
N_2	*IV*	*Fire*	*19*	*467*	*488*	*At about 1 m: 2.5 bar[(1)]*	
He	*IV*	*Fire*	*19*	*700*	*730*	*At about 1 m: 4.5 bar[(1)]*	
He	*IV*	*Fire*	*19*	*467*	*506*	*At about 1 m: 2.5 bar[(1)]*	
H_2	*IV*	*Fire*	*19*	*700*	*713*	*At about 1 m: 450 mbar[(1)]*	
H_2	*IV*	*Fire*	*19*	*467*	*483*	*At about 1 m: 6-7 bar[(1)]*	

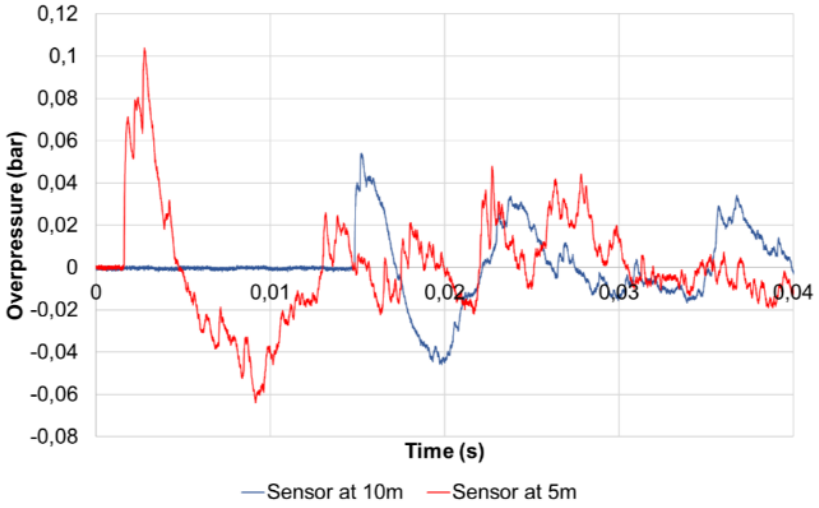

Fig. 2. *Pressure signals measured for the burst of a 2.4 L bottle containing 700 bar of hydrogen. Red: at 5 m. Blue: at 10 m.*

Again, a campaign only supplies a single measurement, which is not enough for testing the codes. This measurement can also be disturbed by the surrounding walls. The data coming from (INERIS, 2010) presents several tests and two measuring points. The first pressure rise is followed by several pressure peaks. This may notably be explained by a progressive pressure discharge, which is tricky to address through numerical modelling. The first part of the signals of Zalosh et al. (2005) and Tamura (2006) (not shown) is closer to the typical shock wave shape, with a single peak followed by a pressure decay. Some data obtained for non-reacting gases could greatly improve the database, when thinking of modeling tool assessment.

2. Modeling burst tank cases

2.1 Phenomenological tools for free-field bursting tanks

As experimental data appear to miss to provide a complete validation database for CFD dedicated to bursting tanks, some phenomenological tools are regarded. Indeed, if they are accurate enough, they could be used to complete experimental dataset with extra points.

The considered tools are PROJEX, the TNT equivalent (TM5 1300, 1969) and the Baker methods (Baker et al., 1983). Also, the Brode energy upon which PROJEX and the TNT equivalent method rely can be quantified with the ideal gas law and with a real gas law, such as the Able-Nobel one (Molkov et al., 2015). The dataset provided by Zalosh and Tamura is used to test the phenomenological approaches (see Tables 3 and 4). All approaches are employed for a charge located on the ground and do not account for chemical effects related to a fireball generation.

***Table 3**. Phenomenological tools results compared to Zalosh measurements (Zalosh et al., 2005). The Baker method results are from Molkov et al. (2015). Computations made for a TNT equivalent of 4.57 MJ/kg.*

Location	Exp. data	PROJEX (6.46 MJ)	PROJEX A-N (5.33 MJ)	TNT Eq. (1.41 kg)	TNT Eq. A-N (1.16 kg)	BAKER A-N (9.4 MJ)
at 1.9 m orthogonally to the bottle axis	3 bar	2.35 bar	2.05 bar	4.2 bar	3,6 bar	3,19 bar
at 4.2 m on the bottle axis	650 mbar	441 mbar	403 mbar	740 mbar	650 mbar	608 mbar
at 4.2 m orthogonally	830 mbar					
at 6.5 m orthogonally	410 mbar	222 mbar	205 mbar	336 mbar	302 mbar	284 mbar

***Table 4.** Phenomenological tools results compared to Tamura measurements (2006).*

	Location	Exp. data	PROJEX (8.3 MJ)	PROJEX A-N (5.8 MJ)	TNT Eq (1.81 kg)	TNT Eq. A-N (1.27 kg)
35 L type IV bottle	at 5 m orthogonally to the bottle axis	1.1 bar	390 mbar	320 mbar	618 mbar	500 mbar
	at 10 m orthogonally to the bottle axis	234 mbar	138 mbar	116 mbar	196 mbar	165 mbar
		Exp. data	PROJEX (8.95 MJ)	PROJEX A-N (6.3 MJ)	TNT Eq. (1.96 kg)	TNT Eq. A-N (1.37 kg)
36 L type III bottle	at 5 m orthogonally to the bottle axis	743 mbar	402 mbar	331 mbar	650 mbar	520 mbar
	at 10 m orthogonally to the bottle axis	234 mbar	142 mbar	120 mbar	204 mbar	172 mbar

For the Zalosh database, all the methods recover the proper orders of magnitude. Nevertheless, the most accurate methods seem to be the TNT Equivalent method with a real gas law and the Baker method. Concerning the Tamura cases, PROJEX and the TNT equivalent method underestimate the peak about 1 bar, 5 m from the first bottle. Overall, the best results are obtained with the TNT equivalent method.

According to the results, the phenomenological methods give most of the time the proper orders of magnitude when compared with the chosen experiments but are not necessarily accurate. These methods can help to assess a result obtained with CFD but do not give strict reference results.

2.2 CFD

The CFD approach is regarded in modeling the fictitious case of the burst of a 78 L reservoir containing air at a pressure of 610 bar. The CFD tool is OpenFoam (Weller, 1998). The solver *rhoCentralFoam* is chosen. It solves the Euler equations with the convective numerical scheme of Kurganov and Tadmor (2000). The time derivatives are discretized with the Euler scheme. The basic solver does not account for transport equations for the chemical species, meaning the gas in the bottle and in the environment is the same. By default, also, the user can only rely on an ideal gas law. The specific heat at constant pressure can be set to a constant or a JANAF table can be used to introduce a law $C_p = C_p(T)$.

Developments were carried out to add the transport equations for chemical species and enable to account for a real gas law such as the Peng-Robinson one. A recent work (Ghasemi, 2020) gives elements to perform the coding.

Several CFD computations are performed for a regular mesh, the cell width being 5 cm. In a volume equal to the tank one, a pressure of 610 bar is initially imposed. The discharge is then implicitly modeled as the instantaneous disappearance of the tank walls. The results of the CFD computations for several parametrizations are given in the Table below, as well as results obtained with phenomenological tools. It can be seen these latter tools provide the same orders of magnitude from 5 to 30 m from the pressure source, the TNT equivalent overpredicting the PROJEX results. In the previous part, the TNT equivalent gave the best results for similar bursting cases. The CFD computation based on a resolution of the chemical species transport equations and a real gas law gave the closest results to the TNT equivalent ones. It should be nevertheless noted that in the previous part, the regarded cases involved a fireball, that potentially contributed to pressure effects and not the current one.

***Table 5**. Pressure effects at several distances related to a fictitious case of a bursting 78 L reservoir containing 610 bar of air. Several computing methods are used.*

	Distance (m)					
Modeling method	5	10	15	20	25	30
PROJEX (E=12.2 MJ)	472 mbar	162 mbar	93 mbar	65 mbar	51 mbar	41 mbar
TNT equivalent (m=2.67 kg)	795 mbar	238 mbar	133 mbar	91 mbar	70 mbar	55 mbar
CFD with ideal gas law and constant Cp coefficients	168 mbar	69 mbar	38 mbar	25 mbar	21 mbar	19 mbar
CFD with transport equations for chemical species, an ideal gas law and JANAF tables	1550 mbar	320 mbar	189 mbar	154 mbar	124 mbar	90 mbar
CFD with transport equations for chemical species, a real gas law (Peng-Robinson) and JANAF tables	823 mbar	237 mbar	155 mbar	109 mbar	94 mbar	84 mbar

Finally, first CFD computations of a case of the Kudriakov et al. campaign is performed. The Helium case is addressed as it is theoretically the simplest as no fireball is generated at the tank rupture. The computational domain is 3D and 120 m long. It is decomposed into cubic cells with a characteristic width of 5 cm.

It was chosen to work with relatively small cells instead of using an Automatic Mesh Refinement (AMR) method. Indeed, the criterion that is used by default is the normalized pressure gradient meaning only the first pressure wave will be refined. This may be fine for dealing with free field cases but not necessarily tunnel cases for which the reflection zone involving numerous pressure waves is of importance.

Two CFD simulations are performed, both with the transport of the chemical species and JANAF tables for computing the Cp coefficients. The first CFD relies on the ideal gas law, the other on the Peng-Robinson law.

The Figure 4 shows the results obtained 30 m away from the pressure source and the measured pressure signal. It should be pointed out the experimental signal presented in the Kudriakov et al. paper has been treated with a low-pass filter and a cut-off frequency of 100 Hz to suppress acoustic effects. This signal as well as the unfiltered one are given in the Figure. It can be seen the shocks disappeared with the filtering procedure. The CFD results are very similar between them. The impact of the gas law can be noticed, as the real gas law leads to lower pressure magnitude but remains moderate. The CFD pressure waves have a higher intensity than the experimental one and are quicker. These computations are first attempts in order to assess their potential, but extra work is needed to address properly free field cases.

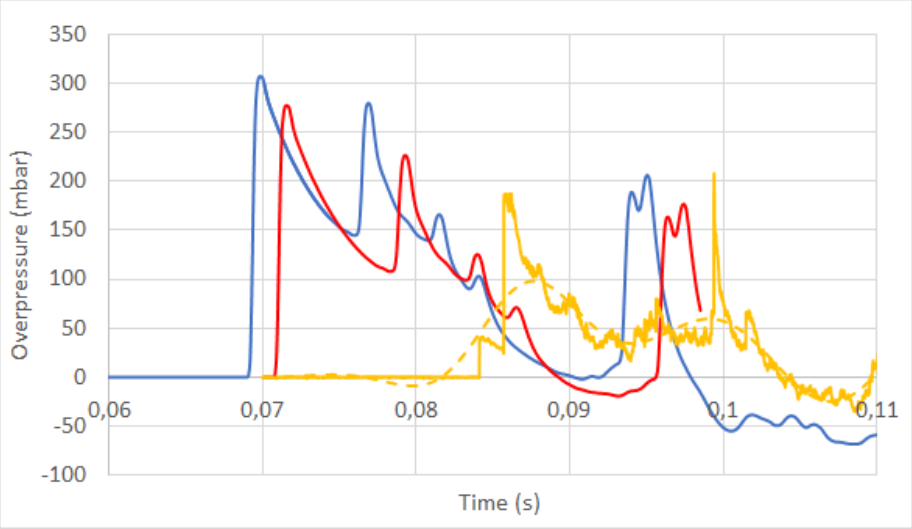

Fig. 3. *Experimental (yellow) raw (line) and filtered (dash line) signal measured at 30 m after bursting of a 78 L Helium bottle under 650 bar in the Mortier tunnel (Kudriakov et al., 2022). CFD modelling with an ideal gas law (blue) and a real gas law (red).*

3. Conclusions

A CFD approach is studied for dealing with high-pressure tank burst in tunnels. Reference tests are needed to propose a CFD strategy. Most tests are physically complex as they correspond to a thermal aggression of a hydrogen tank. These tests do not permit to quantify the part of pressure effects related to the fireball and the other one related to gas expansion.

Tests in tunnels were performed but the available data remain too limited to design and validate step by step a CFD modeling strategy. A promising experimental campaign could consist in provoking tank burst in free field for one or two non-reacting gas and for hydrogen, for the same tank volume and the same initial pressure. Burst could be generated by a detonating cord to control the discharge mode (initial pressure and surface discharging pressure). Repeatability tests would be needed. The same tests could be performed in a gallery or in a tunnel. The locations of the pressure probes should be the same in both types of tests and chosen in order to detect in tunnel, the reflection zone, the planar zone and the transition between the two of them.

Phenomenological tools were tested against some free field results. These models recover orders of magnitude for the pressure magnitude but their accuracy may vary. The way the pressure energy is quantified for high pressure cases may impact the results.

Some CFD was performed in free field and in tunnel. Some modeling choices for thermodynamics seem to be preferable nevertheless, the results obtained in the tunnel overestimate the experimental results. Extra work is needed based on the analysis of the projected experimental campaign mentioned above. This latter could also be beneficial for checking the behavior of already existing CFD strategies for modeling hydrogen tank bursts (Molkov et al., 2021).

Acknowledgements

The authors wish to thank Sergey Kudriakov for providing the unfiltered pressure signal related to the Helium tank rupture in the Mortier tunnel.

References

Kudriakov, S. et al., 2022. Full-scale tunnel experiments: Blast wave and fireball evolution following hydrogen tank rupture. Int. J. Hydrogen Energy 47(43), pp. 18911-18933

Blanc-Vannet, P. et al., 2019. Fire tests carried out in FCH JU Firecomp project, recommendations and application to safety of gas storage systems, Int. J. of Hydrogen Energy 44(17), pp. 9100-9109

Ruban, S. et al., 2012. Fire risk on high-pressure full composite cylinders for automotive applications, Int. J. of Hydrogen Energy 37 pp. 17630-17638

INERIS test campaign, 2012 (no publication)

Molkov, V. et al., 2015. Blast wave from a high-pressure tank rupture in a fire: Stand-alone and under-vehicle hydrogen tanks, Int. J. of Hydrogen Energy 40, pp. 12581-12603

Molkov, V.V. et al., 2021. Dynamics of blast wave and fireball after hydrogen tank rupture in a fire in the open atmosphere. Int. J. Hydrogen Energy 46(5), pp. 4644-4665

Brode, H.L., 1959. Blast waves from a spherical charge. Phys Fluids 2, pp. 217-29

Heudier, L., 2013. Les éclatements de capacité. Phénoménologie et modélisation des effets. Rapport Omega 15. www.ineris.fr.

Van den Berg, A.C., 1984. The Multi-Energy method – a framework for vapour cloud explosion blast prediction, TNO-PML Report 1984-C72

Zalosh, R. et al., 2005. Hydrogen Fuel Tank Fire Exposure Burst Test. SAE 2005-01-1886

Shen, C. et al., 2018. Consequence assessment of high-pressure hydrogen storage tank rupture during fire test. J. Loss Prev. in the Process Ind. 55, pp. 223-231

Tamura, Y. et al., 2006. Fire exposure burst test of 70MPa automobile high-pressure hydrogen cylinders. Society of Automotive Engineers of Japan Annual Autumn Congress

Chaineaux, J. et al., 2000. Sûreté des dispositifs de stockage de l'hydrogène sous haute pression équipant des véhicules routiers. Final report. EURO-QUEBEC HYDRO-HYDROGENE Project.

INERIS test campaign, 2010 (no publication).

TM5 1300, 1969. Department of the Army, the Navy and the Air Force. Structures to resist the effects of accidental explosions. Technical Manual, NAFVAC-P397 / AFM88

Baker, W.E., Cox, P.A., Westine, J.J., Kulesz, R.A., Strehlow, P.S., 1983. Explosion hazards and evaluation, Elsevier editions.

Weller, H.G, Tabor, G., 1998. A tensorial approach to computational continuum mechanics using object-oriented techniques. Computational Physics 12, pp. 620-631.

Kurganov, A. et al., 2000, New High-Resolution Central Schemes for Nonlinear Conservation Laws and Convection–Diffusion Equations, Journal of Computational Physics 160, pp. 241-282

Ghasemi, K.A., 2020. Release of high-pressure hydrogen into the air, Master's Thesis, University of South-Eastern Norway